

A NEW KOHN-VOGELIUS TYPE FORMULATION FOR INVERSE SOURCE PROBLEMS

XIAOLIANG CHENG

Department of Mathematics, Zhejiang University
Hangzhou, Zhejiang 310027, China

RONGFANG GONG*

Department of Mathematics, Nanjing University of Aeronautics and Astronautics
Nanjing, Jiangsu 210016, China

WEIMIN HAN

Department of Mathematics, University of Iowa
Iowa City, IA 52242, USA

(Communicated by Fioralba Cakoni)

ABSTRACT. In this paper we propose a Kohn-Vogelius type formulation for an inverse source problem of partial differential equations. The unknown source term is to be determined from both Dirichlet and Neumann boundary conditions. We introduce two different boundary value problems, which depend on two different positive real numbers α and β , and both of them incorporate the Dirichlet and Neumann data into a single Robin boundary condition. This allows noise in both boundary data. By using the Kohn-Vogelius type Tikhonov regularization, data to be fitted is transferred from boundary into the whole domain, making the problem resolution more robust. More importantly, with the formulation proposed here, satisfactory reconstruction could be achieved for rather small regularization parameter through choosing properly the values of α and β . This is a desirable property to have since a smaller regularization parameter implies a more accurate approximation of the regularized problem to the original one. The proposed method is studied theoretically. Two numerical examples are provided to show the usefulness of the proposed method.

1. Introduction. Let $\Omega \subset \mathbb{R}^d$ ($d \leq 3$: space dimension) be an open bounded set with a Lipschitz boundary Γ , and let $\Omega_0 \subset \Omega$ be a Lipschitz subset. We consider the following inverse source problem: Given g_1 and g_2 on Γ , find p such that the solution of boundary value problem (BVP)

$$(1) \quad \begin{cases} -\Delta u + u = p\chi_{\Omega_0} & \text{in } \Omega, \\ \frac{\partial u}{\partial n} = g_2 & \text{on } \Gamma \end{cases}$$

satisfies

$$(2) \quad u = g_1 \quad \text{on } \Gamma.$$

Here $\frac{\partial}{\partial n}$ is the outward normal derivative, and χ_{Ω_0} is the characteristic function of Ω_0 , i.e., its value is 1 in Ω_0 while 0 outside Ω_0 . In the context of applications

2010 *Mathematics Subject Classification.* Primary: 65N21, 65F22; Secondary: 49J40.

Key words and phrases. Inverse source problems, Tikhonov regularization, Kohn-Vogelius type functional, error estimates, iterative methods.

* Corresponding author: Rongfang Gong.

in bioluminescence tomography, Ω_0 is known as a permissible region of the source function p .

It is well known that inverse source problems are under-determined and ill-posed. In this paper, we consider using Tikhonov regularization [9, 13] to obtain a stable approximate solution for the inverse source problem associated with the BVP (1). We note that the inverse source problem (1)–(2) has been studied extensively through Tikhonov methods in the field of bioluminescence tomography, see e.g. [7, 8, 11] and references therein. With the Tikhonov regularization, the original inverse source problem (1)–(2) is converted to the following minimization problem:

$$(3) \quad p_\varepsilon = \arg \min_{p \in Q_{ad}} \frac{1}{2} \|u(p) - g_1\|_{0,\Gamma}^2 + \frac{\varepsilon}{2} \|p\|_{0,\Omega_0}^2, \quad \varepsilon > 0,$$

where $Q_{ad} \subset Q := L^2(\Omega_0)$ is an admissible set, incorporating a priori information about the source function p ; for each $p \in Q$, $u(p)$ is the weak solution of the BVP (1) in the Sobolev space $V := H^1(\Omega)$; $\|\cdot\|_{0,\Gamma}$ and $\|\cdot\|_{0,\Omega_0}$ are standard norms of the spaces $L^2(\Gamma)$ and $L^2(\Omega_0)$. Under some assumptions, Problem (3) admits a unique solution p_ε , and as $\varepsilon \rightarrow 0$, p_ε converges to p^* , a solution of (1)–(2) with minimal L^2 -norm ([7]).

In [12], a Kohn-Vogelius type functional is used for the data fitting in solving the inverse source problem. In general, Kohn-Vogelius functionals are expected to lead to more robust optimization procedures [1]. For the inverse problem (1)–(2), the formulation studied in [12] is

$$(4) \quad p_\varepsilon = \arg \min_{p \in Q_{ad}} \frac{1}{2} \|u_1(p) - u_2(p)\|_{0,\Omega}^2 + \frac{\varepsilon}{2} \|p\|_{0,\Omega_0}^2, \quad \varepsilon > 0,$$

where $u_1(p), u_2(p) \in V$ are the weak solutions of BVPs

$$\begin{cases} -\Delta u_1 + u_1 = p\chi_{\Omega_0} & \text{in } \Omega, \\ u_1 = g_1 & \text{on } \Gamma, \end{cases}$$

and

$$\begin{cases} -\Delta u_2 + u_2 = p\chi_{\Omega_0} & \text{in } \Omega, \\ \frac{\partial u_2}{\partial n} = g_2 & \text{on } \Gamma, \end{cases}$$

respectively; $\|\cdot\|_{0,\Omega}$ is the standard $L^2(\Omega)$ norm. Under certain assumptions, Problem (4) admits a unique stable solution p_ε which converges to p^* ([12]).

The regularization parameter ε plays an important role in solution accuracy and stability. In this paper, we propose a new Kohn-Vogelius type functional to solve the inverse source problem which allows the use of very small values of the parameter ε . Consequently, we can compute accurate approximations of the solution corresponding to rather small ε . This is a desirable property since the smaller the regularization parameter, the better the approximation of the regularized problem to the original one. Moreover, with introduction of two positive real parameters, boundary condition data and boundary measurement data can be incorporated into a single boundary value condition, and this improves the stability of the solution with respect to the noise in the data. Moreover, data to be fitted is transferred from boundary into the whole domain, making the problem resolution more robust.

The structure for the rest of this paper is as follows. The new Kohn-Vogelius type method is proposed for the problem (1)–(2) in section 2. Some theoretical properties are shown in this section. We discuss in section 3 the model when the data contains random noise, and a convergence result is proved. In section 4, we provide a direct study of a system that defines the source function from

the regularized formulations, with or without the noise. In section 5, an iterative algorithm is stated for practical reconstructions. Its convergence is ensured when the two parameters α and β are sufficiently close. Several numerical examples are presented in section 6 to demonstrate the feasibility and efficiency of the proposed method. Finally, concluding remarks are given in section 7.

2. A new Kohn-Vogelius type method. Let $\alpha \neq \beta$ be two positive constants. Consider the following two BVPs:

$$(5) \quad \begin{cases} -\Delta u_1 + u_1 = p\chi_{\Omega_0} & \text{in } \Omega, \\ \frac{\partial u_1}{\partial n} + \alpha u_1 = g_2 + \alpha g_1 & \text{on } \Gamma, \end{cases}$$

and

$$(6) \quad \begin{cases} -\Delta u_2 + u_2 = p\chi_{\Omega_0} & \text{in } \Omega, \\ \frac{\partial u_2}{\partial n} + \beta u_2 = g_2 + \beta g_1 & \text{on } \Gamma. \end{cases}$$

Then the inverse source problem (1)–(2) can be transferred to the one of finding a p such that the solution u_1 of (5) and the solution u_2 of (6) are equal: $u_1 = u_2$ in Ω . Indeed, if (u, p) satisfy (1)–(2), then (5) and (6) follow immediately with $u_1 = u_2 = u$. Conversely, if there is a p such that the solutions of (5) and (6) satisfy $u_1 = u_2$ in Ω , we subtract the two boundary conditions to have $(\beta - \alpha)(u_1 - g_1) = 0$ on Γ , implying $u_1 = g_1$ on Γ since $\beta \neq \alpha$. Substitute $u_1 = g_1$ back into (5) to get $\frac{\partial u_1}{\partial n} = g_2$ on Γ . Therefore, $(u_1, p) (= (u_2, p))$ satisfy (1)–(2).

Based on the two BVPs (5) and (6), we give a new Kohn-Vogelius type method for the inverse source problem. Following the idea of Tikhonov regularization, we define a Kohn-Vogelius type objective functional

$$J_\varepsilon(p) = \frac{1}{2} \|u_1(p) - u_2(p)\|_{1,\Omega}^2 + \frac{\varepsilon}{2} \|p\|_{0,\Omega_0}^2,$$

where $u_1(p), u_2(p) \in V$ are the weak solutions of BVPs (5) and (6), respectively; $\|\cdot\|_{1,\Omega} = (\|\nabla \cdot\|_{0,\Omega}^2 + \|\cdot\|_{0,\Omega}^2)^{1/2}$; ε is a regularization parameter. Assuming $g_1, g_2 \in H^{-1/2}(\Gamma)$, it follows from the Lax-Milgram lemma ([2, 5]) that for each $p \in Q$, the solutions $u_1, u_2 \in V$ exist and are unique. Here $H^{-1/2}(\Gamma)$ is the dual of $H^{1/2}(\Gamma)$ ([10, Chapter I]).

Compared with the original fitting condition (2): $u(p) = g_1$ on Γ , the new fitting condition $u_1(p) = u_2(p)$ in Ω appears to make the problem less under-determined. Moreover, the regularity assumption on g_1 is $g_1 \in H^{-1/2}(\Gamma)$ rather than $g_1 \in H^{1/2}(\Gamma)$; note that for noisy measurement data, we only have $g_1 \in L^2(\Gamma)$, not $g_1 \in H^{1/2}(\Gamma)$. Also, it is rather direct to calculate the term $\|u_1(p) - u_2(p)\|_{1,\Omega}$. For $\|u(p) - g_1\|_{0,\Gamma}$, we need to use values of $u(p)$ on Γ ; in the case of a general curved boundary, it is a rather delicate issue to calculate $\|u(p) - g_1\|_{0,\Gamma}$ accurately.

The source function is sought within an admissible set Q_{ad} , assumed to be a closed convex subset of Q . We introduce the following regularized problem.

Problem 1. Find $p_\varepsilon \in Q_{ad}$ such that

$$(7) \quad J_\varepsilon(p_\varepsilon) = \inf_{p \in Q_{ad}} J_\varepsilon(p).$$

Regarding Problem 1, we have the following well-posedness results.

Proposition 1. For $\varepsilon > 0$, Problem 1 admits a unique solution $p_\varepsilon \in Q_{ad}$, which depends continuously on $g_1, g_2 \in H^{-1/2}(\Gamma)$ and ε . The following first order necessary

and sufficient condition for p_ε holds:

$$(8) \quad \int_{\Omega_0} (\varepsilon p_\varepsilon - (\alpha \Phi_1 - \beta \Phi_2)) (q - p_\varepsilon) dx \geq 0 \quad \forall q \in Q_{ad},$$

where $\Phi_1, \Phi_2 \in V$ are weak solutions of the adjoint BVPs

$$(9) \quad \begin{cases} -\Delta \Phi_1 + \Phi_1 = 0 & \text{in } \Omega, \\ \frac{\partial \Phi_1}{\partial n} + \alpha \Phi_1 = u_1(p_\varepsilon) - u_2(p_\varepsilon) & \text{on } \Gamma, \end{cases}$$

and

$$(10) \quad \begin{cases} -\Delta \Phi_2 + \Phi_2 = 0 & \text{in } \Omega, \\ \frac{\partial \Phi_2}{\partial n} + \beta \Phi_2 = u_1(p_\varepsilon) - u_2(p_\varepsilon) & \text{on } \Gamma, \end{cases}$$

respectively.

Proof. It is not difficult to verify that for $\varepsilon > 0$, $J_\varepsilon(\cdot)$ is strictly convex on Q . Because Q_{ad} is a convex and closed subset of space Q , it is a standard result ([2, 10]) that Problem 1 admits a unique solution $p_\varepsilon \in Q_{ad}$, depending continuously on $g_1, g_2 \in H^{-1/2}(\Gamma)$ and $\varepsilon > 0$, and is characterized by the inequality

$$(11) \quad J'_\varepsilon(p_\varepsilon) (q - p_\varepsilon) \geq 0 \quad \forall q \in Q_{ad}.$$

Next we derive an equivalent formulation for (11). For any $q \in Q$, we consider the auxiliary BVPs:

$$(12) \quad \begin{cases} -\Delta w_1 + w_1 = q \chi_{\Omega_0} & \text{in } \Omega, \\ \frac{\partial w_1}{\partial n} + \alpha w_1 = 0 & \text{on } \Gamma, \end{cases}$$

and

$$(13) \quad \begin{cases} -\Delta w_2 + w_2 = q \chi_{\Omega_0} & \text{in } \Omega, \\ \frac{\partial w_2}{\partial n} + \beta w_2 = 0 & \text{on } \Gamma. \end{cases}$$

Then for any $t \in \mathbb{R}$, the solutions $u_1(p_\varepsilon + tq)$, $u_2(p_\varepsilon + tq)$ of (5), (6) (p replaced by $p_\varepsilon + tq$) equal to $u_1(p_\varepsilon) + tw_1(q)$, $u_2(p_\varepsilon) + tw_2(q)$, respectively. Therefore, the Gateaux derivative of J_ε at p_ε in the direction $q \in Q$ is

$$\begin{aligned} J'_\varepsilon(p_\varepsilon) q &= \lim_{t \rightarrow 0} \frac{J_\varepsilon(p_\varepsilon + tq) - J_\varepsilon(p_\varepsilon)}{t} \\ &= \int_{\Omega} [\nabla(u_1(p_\varepsilon) - u_2(p_\varepsilon)) \cdot \nabla(w_1(q) - w_2(q)) \\ &\quad + (u_1(p_\varepsilon) - u_2(p_\varepsilon)) \cdot (w_1(q) - w_2(q))] dx + \varepsilon \int_{\Omega_0} p_\varepsilon q dx. \end{aligned}$$

By using integration by parts together with the definitions of $w_1(q)$, $w_2(q)$, Φ_1 and Φ_2 , the above expression reduces to

$$J'_\varepsilon(p_\varepsilon) q = \int_{\Omega_0} (\varepsilon p_\varepsilon - (\alpha \Phi_1 - \beta \Phi_2)) q dx;$$

Thus, (8) follows from (11). The proof is completed. \square

Throughout this paper, we assume that there is at least one solution to the original noise-free inverse source problem (1)–(2), and denote by $S \subset Q$ the set of all the solutions, which is also the solution set of Problem 1 with $\varepsilon = 0$. It is not difficult to verify that S is closed and convex. Denote by p^* the unique element in S with minimal L^2 -norm. Since

$$J_\varepsilon(p_\varepsilon) \leq J_\varepsilon(p^*) = \frac{1}{2} \varepsilon \|p^*\|_{0, \Omega_0}^2,$$

we have

$$\|p_\varepsilon\|_{0,\Omega_0} \leq \|p^*\|_{0,\Omega_0}.$$

Then with arguments similar to those in [7, Proposition 3.5], we have the following limiting property.

Proposition 2. $p_\varepsilon \rightarrow p^*$ in Q as $\varepsilon \rightarrow 0^+$.

The optimality condition (8) is equivalent to a nonlinear equation

$$(14) \quad p_\varepsilon = P_{Q_{ad}}\left(\frac{1}{\varepsilon}(\alpha\Phi_1 - \beta\Phi_2)\right),$$

where $P_{Q_{ad}}$ is a orthogonal projection from Q onto Q_{ad} .

On the function $\frac{1}{\varepsilon}(\alpha\Phi_1 - \beta\Phi_2)$, we have the following result.

Proposition 3. Fix α and take $\beta = \alpha + O(\sqrt{\varepsilon})$. Then $\frac{1}{\varepsilon}(\alpha\Phi_1 - \beta\Phi_2)$ is uniformly bounded in V with respect to ε for small $\varepsilon > 0$.

Proof. Denote by $u_1, u_2 \in V$ the weak solutions of (5) and (6) respectively, both with p replaced by p_ε . From the regularity estimate of elliptic BVPs ([6]), we have

$$(15) \quad \begin{aligned} \|u_1\|_{1,\Omega} &\leq c(\|p_\varepsilon\|_{0,\Omega_0} + \|g_2 + \alpha g_1\|_{-1/2,\Gamma}) \\ &\leq c(\|p^*\|_{0,\Omega_0} + \alpha\|g_1\|_{-1/2,\Gamma} + \|g_2\|_{-1/2,\Gamma}) \leq c. \end{aligned}$$

The difference function $\delta u = u_2 - u_1$ satisfies

$$(16) \quad \begin{aligned} &\int_{\Omega} (\nabla\delta u \cdot \nabla v + \delta u v) dx + \beta \int_{\Gamma} \delta u v ds \\ &= (\alpha - \beta) \int_{\Gamma} u_1 v ds + (\beta - \alpha) \int_{\Gamma} g_1 v ds \quad \forall v \in V. \end{aligned}$$

Taking $v = \delta u$ in (16) and using (15), we get

$$(17) \quad \|\delta u\|_{1,\Omega} \leq c|\beta - \alpha|(\|u_1\|_{-1/2,\Gamma} + \|g_1\|_{-1/2,\Gamma}) \leq c|\beta - \alpha|.$$

Similarly, from definition of Φ_1 in (9) and Φ_2 in (10),

$$(18) \quad \int_{\Omega} (\nabla\Phi_1 \cdot \nabla v + \Phi_1 v) dx + \alpha \int_{\Gamma} \Phi_1 v ds = - \int_{\Gamma} \delta u v ds \quad \forall v \in V,$$

$$(19) \quad \int_{\Omega} (\nabla\Phi_2 \cdot \nabla v + \Phi_2 v) dx + \beta \int_{\Gamma} \Phi_2 v ds = - \int_{\Gamma} \delta u v ds \quad \forall v \in V.$$

Taking $v = \Phi_1$ in (18) and $v = \Phi_2$ (19), and using (17), we obtain

$$(20) \quad \|\Phi_1\|_{1,\Omega} \leq c|\beta - \alpha|, \quad \|\Phi_2\|_{1,\Omega} \leq c|\beta - \alpha|.$$

The function $\delta\Phi = \Phi_2 - \Phi_1$ satisfies

$$(21) \quad \int_{\Omega} (\nabla\delta\Phi \cdot \nabla v + \delta\Phi v) dx + \beta \int_{\Gamma} \delta\Phi v ds = (\alpha - \beta) \int_{\Gamma} \Phi_1 v ds \quad \forall v \in V.$$

Taking $v = \delta\Phi$ in (21) and using (20) give

$$(22) \quad \|\delta\Phi\|_{1,\Omega} \leq c|\beta - \alpha|\|\Phi_1\|_{-1/2,\Gamma} \leq c|\beta - \alpha|\|\Phi_1\|_{0,\Omega} \leq c(\beta - \alpha)^2.$$

Combine (20) and (22) to give

$$\|\alpha\Phi_1 - \beta\Phi_2\|_{1,\Omega} = \|\alpha\delta\Phi + (\beta - \alpha)\Phi_2\|_{1,\Omega} \leq c(\beta - \alpha)^2$$

Therefore, if $\beta - \alpha = O(\sqrt{\varepsilon})$, then

$$\left\|\frac{1}{\varepsilon}(\alpha\Phi_1 - \beta\Phi_2)\right\|_{1,\Omega} = O(1),$$

and the proof is completed. □

Proposition 3 indicates that a reasonable reconstruction could be achieved for rather small regularization parameter with properly selected α and β . More precisely, $\beta = \alpha + O(\sqrt{\varepsilon})$, and this provides a guidance on how to choose α and β in numerical simulations, cf. Section 6.

3. Noise model and solution convergence. In this section, the discussion focuses on the case where the Dirichlet data g_1 and Neumann data g_2 are allowed to contain random noise. Thus, assume noise data g_1^δ and g_2^δ satisfy

$$(23) \quad \|g_1^\delta - g_1\|_{0,\Gamma} \leq \delta \text{ and } \|g_2^\delta - g_2\|_{0,\Gamma} \leq \delta,$$

where $\delta > 0$ is known as the noise level. Here and below, we make the natural assumption that g_1, g_2, g_1^δ and g_2^δ all belong to the space $L^2(\Gamma)$.

The problem we need to solve is: find a source function p in Q_{ad} so that the weak solution $u_1^\delta = u_1^\delta(p) \in V$ of

$$(24) \quad \begin{cases} -\Delta u_1^\delta + u_1^\delta = p\chi_{\Omega_0} & \text{in } \Omega, \\ \frac{\partial u_1^\delta}{\partial n} + \alpha u_1^\delta = g_2^\delta + \alpha g_1^\delta & \text{on } \Gamma, \end{cases}$$

equals to the weak solution $u_2^\delta = u_2^\delta(p) \in V$ of

$$(25) \quad \begin{cases} -\Delta u_2^\delta + u_2^\delta = p\chi_{\Omega_0} & \text{in } \Omega, \\ \frac{\partial u_2^\delta}{\partial n} + \beta u_2^\delta = g_2^\delta + \beta g_1^\delta & \text{on } \Gamma, \end{cases}$$

i.e., $u_1^\delta(p) = u_2^\delta(p)$ in Ω . A preliminary computation shows that

$$(26) \quad \|u_1^\delta(p) - u_1(p)\|_{1,\Omega} \leq c\delta, \quad \|u_2^\delta(p) - u_2(p)\|_{1,\Omega} \leq c\delta.$$

Similar to the noise-free model, we define a Kohn-Vogelius type objective functional

$$J_\varepsilon^\delta(p) = \frac{1}{2} \|u_1^\delta(p) - u_2^\delta(p)\|_{1,\Omega}^2 + \frac{\varepsilon}{2} \|p\|_{0,\Omega_0}^2,$$

and introduce the following regularized problem.

Problem 2. Find $p_\varepsilon^\delta \in Q_{ad}$ such that

$$J_\varepsilon^\delta(p_\varepsilon^\delta) = \inf_{p \in Q_{ad}} J_\varepsilon^\delta(p).$$

Remark 1. In the ordinary Tikhonov regularization, noisy measurements are only used in objective functional for data fitting. In our framework here, noisy data, including both Dirichlet and Neumann type, are used in defining the forward problems.

Similar to Problem 1, for $\varepsilon > 0$, Problem 2 admits a unique solution $p_\varepsilon^\delta \in Q_{ad}$, which depends continuously on boundary data g_1^δ, g_2^δ and parameter ε . Thus $p_\varepsilon^\delta \rightarrow p_\varepsilon$ in Q as $\delta \rightarrow 0$. Moreover, similar to (8) and (14), both the first order necessary and sufficient condition of p_ε^δ ,

$$\int_{\Omega_0} (\varepsilon p_\varepsilon^\delta - (\alpha\Phi_1^\delta - \beta\Phi_2^\delta)) (q - p_\varepsilon^\delta) dx \geq 0 \quad \forall q \in Q_{ad}$$

and the nonlinear projection equation,

$$(27) \quad p_\varepsilon^\delta = P_{Q_{ad}} \left(\frac{1}{\varepsilon} (\alpha\Phi_1^\delta - \beta\Phi_2^\delta) \right)$$

hold. Here $\Phi_1^\delta, \Phi_2^\delta \in V$ are the weak solutions of

$$(28) \quad \begin{cases} -\Delta \Phi_1^\delta + \Phi_1^\delta = 0 & \text{in } \Omega, \\ \frac{\partial \Phi_1^\delta}{\partial n} + \alpha \Phi_1^\delta = u_1^\delta(p_\varepsilon^\delta) - u_2^\delta(p_\varepsilon^\delta) & \text{on } \Gamma, \end{cases}$$

and

$$(29) \quad \begin{cases} -\Delta \Phi_2^\delta + \Phi_2^\delta = 0 & \text{in } \Omega, \\ \frac{\partial \Phi_2^\delta}{\partial n} + \beta \Phi_2^\delta = u_1^\delta(p_\varepsilon^\delta) - u_2^\delta(p_\varepsilon^\delta) & \text{on } \Gamma, \end{cases}$$

respectively.

Recall that we always assume exact measurement g_1 is attainable. Therefore the solution set S of the original noise-free problem is non-empty and p^* , the exact solution with minimum norm, exists. Next we discuss the convergence of p_ε^δ to p^* as the noise level $\delta \rightarrow 0$.

Proposition 4. *Given a sequence of noise levels $\{\delta_n\}_{n \geq 1}$, $\delta_n \rightarrow 0$ as $n \rightarrow \infty$, let $\varepsilon_n = \varepsilon(\delta_n)$ be chosen satisfying $\varepsilon_n \rightarrow 0$ and $\delta_n^2/\varepsilon_n \rightarrow 0$, as $n \rightarrow \infty$. Denote by $p_{\varepsilon_n}^{\delta_n} \in Q_{ad}$ the solution of Problem 2 with g_1^δ, g_2^δ and ε replaced by $g_1^{\delta_n}, g_2^{\delta_n}$ and ε_n respectively. Then the sequence $\{p_{\varepsilon_n}^{\delta_n}\}_{n \geq 0}$ converges to p^* as $n \rightarrow \infty$.*

Proof. For simplicity in exposition, write $p^n = p_{\varepsilon_n}^{\delta_n}$, $g_1^n = g_1^{\delta_n}$ and $g_2^n = g_2^{\delta_n}$. Moreover, denote by $u_1^n = u_1^{\delta_n}(p^n)$ and $u_2^n = u_2^{\delta_n}(p^n)$ the unique weak solutions of (24) and (25) in V respectively, both with p, g_1^δ and g_2^δ replaced by p^n, g_1^n and g_2^n . From the definition of p^* , we have $u_1(p^*) = u_2(p^*)$, $\Phi_1(p^*) = \Phi_2(p^*) = 0$. Then, using (26),

$$J_{\varepsilon_n}^{\delta_n}(p^n) \leq J_{\varepsilon_n}^{\delta_n}(p^*) = \frac{1}{2} \|u_1^n(p^*) - u_2^n(p^*)\|_{1,\Omega}^2 + \frac{\varepsilon_n}{2} \|p^*\|_{0,\Omega_0}^2 \leq c \delta_n^2 + \frac{1}{2} \varepsilon_n \|p^*\|_{0,\Omega_0}^2$$

which implies that for n large enough,

$$(30) \quad \|p^n\|_{0,\Omega_0}^2 \leq c \frac{\delta_n^2}{\varepsilon_n} + \|p^*\|_{0,\Omega_0}^2.$$

From the regularity bound of elliptic BVPs,

$$(31) \quad \begin{aligned} \|u_1^n\|_{1,\Omega} &\leq c (\|p^n\|_{0,\Omega_0} + \|g_1^n\|_{0,\Gamma} + \|g_2^n\|_{0,\Gamma}) \\ &\leq c (\|p^n\|_{0,\Omega_0} + 2\delta_n + \|g_1\|_{0,\Gamma} + \|g_2\|_{0,\Gamma}). \end{aligned}$$

Similarly,

$$(32) \quad \|u_2^n\|_{1,\Omega} \leq c (\|p^n\|_{0,\Omega_0} + 2\delta_n + \|g_1\|_{0,\Gamma} + \|g_2\|_{0,\Gamma}).$$

Therefore, from (30)–(32), $\{p^n, u_1^n, u_2^n\}$ is uniformly bounded with respect to n in $Q \times V \times V$, and there is a subsequence $\{n'\}$ of the sequence $\{n\}$, and some elements $p^\infty \in Q_{ad}, u_1^\infty, u_2^\infty \in V$ such that as $n' \rightarrow \infty$,

$$(33) \quad \begin{aligned} p^{n'} &\rightharpoonup p^\infty \text{ in } Q, & u_1^{n'} &\rightharpoonup u_1^\infty, u_2^{n'} \rightharpoonup u_2^\infty \text{ in } V \\ u_1^{n'} &\rightarrow u_1^\infty, u_2^{n'} \rightarrow u_2^\infty \text{ in } L^2(\Omega), & u_1^{n'} &\rightarrow u_1^\infty, u_2^{n'} \rightarrow u_2^\infty \text{ in } L^2(\Gamma). \end{aligned}$$

We verify that $u_1^\infty = u_1(p^\infty)$. From the definition of u_1^n , we have

$$(34) \quad \begin{aligned} &\int_{\Omega} (\nabla u_1^{n'} \cdot \nabla v + u_1^{n'} v) dx + \alpha \int_{\Gamma} u_1^{n'} v ds \\ &= \int_{\Omega_0} p^{n'} v dx + \alpha \int_{\Gamma} g_1^{n'} v ds + \int_{\Gamma} g_2^{n'} v ds \quad \forall v \in V. \end{aligned}$$

Let $n' \rightarrow 0$, and use (23) and convergence relations (33) above to get

$$(35) \quad \begin{aligned} & \int_{\Omega} (\nabla u_1^\infty \cdot \nabla v + u_1^\infty v) \, dx + \alpha \int_{\Gamma} u_1^\infty v \, ds \\ &= \int_{\Omega_0} p^\infty v \, dx + \alpha \int_{\Gamma} g_1 v \, ds + \int_{\Gamma} g_2 v \, ds \quad \forall v \in V, \end{aligned}$$

which shows $u_1^\infty = u_1(p^\infty)$. Similarly, we have $u_2^\infty = u_2(p^\infty)$.

Subtracting (35) from (34), taking $v = u_1^{n'} - u_1^\infty$ and using convergence relations in (33) again give to $u_1^{n'} \rightarrow u_1^\infty$ in V as $n' \rightarrow 0$. Similarly, $u_2^{n'} \rightarrow u_2^\infty$ in V as $n' \rightarrow \infty$.

Therefore, as $n' \rightarrow \infty$,

$$J_{\varepsilon_{n'}}^{\delta_{n'}}(p^{n'}) = \frac{1}{2} \|u_1^{n'} - u_2^{n'}\|_{1,\Omega}^2 + \frac{\varepsilon_{n'}}{2} \|p^{n'}\|_{0,\Omega_0}^2 \rightarrow \frac{1}{2} \|u_1^\infty - u_2^\infty\|_{1,\Omega}^2,$$

where we use the uniform boundness of $p^{n'}$ (cf. (30)). Since

$$J_{\varepsilon_{n'}}^{\delta_{n'}}(p^{n'}) \leq J_{\varepsilon_{n'}}^{\delta_{n'}}(p^*) \leq c \delta_{n'}^2 + \frac{\varepsilon_{n'}}{2} \|p^*\|_{0,\Omega_0}^2 \rightarrow 0, \text{ as } n' \rightarrow \infty,$$

we deduce that

$$u_1(p^\infty) = u_2(p^\infty) \text{ in } V.$$

As a result, (p^∞, u_1^∞) or (p^∞, u_2^∞) is a solution of original noise-free inverse source problem (1)–(2). Hence, $p^\infty \in S$.

Next we prove $p^\infty = p^*$. From the lower semi-continuity of norm $\|\cdot\|_{0,\Omega_0}$ and the weak convergence of $p^{n'}$ to p^∞ , we have

$$\|p^\infty\|_{0,\Omega_0} \leq \liminf_{n' \rightarrow \infty} \|p^{n'}\|_{0,\Omega_0}.$$

Therefore, for any fixed $\eta > 0$, there exists a positive integer N such that $\forall n' > N$, the following relation holds:

$$(36) \quad \|p^{n'}\|_{0,\Omega_0}^2 \geq \|p^\infty\|_{0,\Omega_0}^2 - \eta.$$

We note that (30) also holds when p^* is replaced by p^∞ . Therefore, together with (36),

$$-\eta \leq \|p^{n'}\|_{0,\Omega_0}^2 - \|p^\infty\|_{0,\Omega_0}^2 \leq c \frac{\delta_{n'}^2}{\varepsilon_{n'}}$$

holds for big enough $n' > N$. Letting first $n' \rightarrow \infty$ and then $\eta \rightarrow 0$ in the relation above, we have

$$(37) \quad \lim_{n' \rightarrow \infty} \|p^{n'}\|_{0,\Omega_0} = \|p^\infty\|_{0,\Omega_0}.$$

By the definition of p^* , $\|p^*\|_{0,\Omega_0} \leq \|p^\infty\|_{0,\Omega_0}$. Combining it with (30) and (36), for big enough $n' > N$, the following relation holds:

$$\|p^{n'}\|_{0,\Omega_0}^2 - \|p^\infty\|_{0,\Omega_0}^2 \leq \|p^{n'}\|_{0,\Omega_0}^2 - \|p^*\|_{0,\Omega_0}^2 \leq c \frac{\delta_{n'}^2}{\varepsilon_{n'}}$$

Letting $n' \rightarrow \infty$ again in the relation above and using (37), we arrive at

$$(38) \quad \|p^\infty\|_{0,\Omega_0} = \|p^*\|_{0,\Omega_0}.$$

Using the definition of p^* again, (38) means $p^\infty = p^*$ and $p^{n'} \rightharpoonup p^*$ in Q , as $n' \rightarrow \infty$. Thus the limit does not depend on the subsequence selected, and then the entire solution sequence $p^n \rightharpoonup 0$ in Q , as $n' \rightarrow \infty$.

The strong convergence holds due to $\lim_{n \rightarrow \infty} \|p^n\|_{0,\Omega_0} = \|p^*\|_{0,\Omega_0}$ and weak convergence. \square

4. Study of a mapping. From the discussion in sections 2 and 3, we see that the source function from the regularized problem can be equivalently defined by a system: (5), (6), (9), (10) and (14) for the noise-free case, and (24), (25), (28), (29) and (27) for the noise model. The study of the system is the same for either case, and here for simplicity in notation, we consider the noise-free case. To further simplify the notation, we write

$$g_\alpha := g_2 + \alpha g_1, \quad g_\beta := g_2 + \beta g_1.$$

Then, for any $p \in Q_{ad}$, we first define $u_1, u_2 \in V$ by

$$(39) \quad \int_\Omega (\nabla u_1 \cdot \nabla v + u_1 v) dx + \alpha \int_\Gamma u_1 v ds = \int_{\Omega_0} p v dx + \int_\Gamma g_\alpha v ds \quad \forall v \in V,$$

$$(40) \quad \int_\Omega (\nabla u_2 \cdot \nabla v + u_2 v) dx + \beta \int_\Gamma u_2 v ds = \int_{\Omega_0} p v dx + \int_\Gamma g_\beta v ds \quad \forall v \in V,$$

then define $\Phi_1, \Phi_2 \in V$ by

$$(41) \quad \int_\Omega (\nabla \Phi_1 \cdot \nabla v + \Phi_1 v) dx + \alpha \int_\Gamma \Phi_1 v ds = \int_\Gamma (u_1 - u_2) v ds \quad \forall v \in V,$$

$$(42) \quad \int_\Omega (\nabla \Phi_2 \cdot \nabla v + \Phi_2 v) dx + \beta \int_\Gamma \Phi_2 v ds = \int_\Gamma (u_1 - u_2) v ds \quad \forall v \in V,$$

and finally define

$$(43) \quad \Pi(p) = P_{Q_{ad}} \left(\frac{1}{\varepsilon} (\alpha \Phi_1 - \beta \Phi_2) \right).$$

In this way, we have defined a mapping $\Pi : Q_{ad} \rightarrow Q_{ad}$.

We fix $\alpha > 0$ and assume α and β satisfy the relation

$$(44) \quad |\beta - \alpha| \leq c_0 \sqrt{\varepsilon}.$$

We will show that if $c_0 > 0$ is small enough, then the mapping Π is a contraction from Q_{ad} to Q_{ad} . For this purpose, let $p^1, p^2 \in Q_{ad}$ and denote $\delta p = p^1 - p^2$. For $i = 1, 2$, corresponding to p^i , the solutions of (39)–(42) are denoted as u_1^i, u_2^i, Φ_1^i , and Φ_2^i . We denote $\delta u_j = u_j^1 - u_j^2 \in V$ and $\delta \Phi_j = \Phi_j^1 - \Phi_j^2 \in V$ for $j = 1, 2$. Then from the definitions (39)–(42), we have

$$(45) \quad \int_\Omega (\nabla \delta u_1 \cdot \nabla v + \delta u_1 v) dx + \alpha \int_\Gamma \delta u_1 v ds = \int_{\Omega_0} \delta p v dx \quad \forall v \in V,$$

$$(46) \quad \int_\Omega (\nabla \delta u_2 \cdot \nabla v + \delta u_2 v) dx + \beta \int_\Gamma \delta u_2 v ds = \int_{\Omega_0} \delta p v dx \quad \forall v \in V,$$

$$(47) \quad \int_\Omega (\nabla \delta \Phi_1 \cdot \nabla v + \delta \Phi_1 v) dx + \alpha \int_\Gamma \delta \Phi_1 v ds = \int_\Gamma (\delta u_1 - \delta u_2) v ds \quad \forall v \in V,$$

$$(48) \quad \int_\Omega (\nabla \delta \Phi_2 \cdot \nabla v + \delta \Phi_2 v) dx + \beta \int_\Gamma \delta \Phi_2 v ds = \int_\Gamma (\delta u_1 - \delta u_2) v ds \quad \forall v \in V.$$

Take $v = \delta u_1$ in (45) and $v = \delta u_2$ in (46) to get

$$(49) \quad \|\delta u_j\|_{1,\Omega} \leq c \|\delta p\|_{0,\Omega_0}, \quad j = 1, 2.$$

Subtracting (46) from (45), we have, for any $v \in V$,

$$\int_\Omega [\nabla (\delta u_1 - \delta u_2) \cdot \nabla v + (\delta u_1 - \delta u_2) v] dx + \alpha \int_\Gamma (\delta u_1 - \delta u_2) v ds = (\beta - \alpha) \int_\Gamma \delta u_2 v ds.$$

Take $v = \delta u_1 - \delta u_2$ and apply (49) to obtain

$$(50) \quad \|\delta u_1 - \delta u_2\|_{1,\Omega} \leq c |\beta - \alpha| \|\delta u_2\|_{0,\Gamma} \leq c |\beta - \alpha| \|\delta p\|_{0,\Omega_0}.$$

Similarly, take $v = \delta\Phi_1$ in (47), $v = \delta\Phi_2$ in (48) and apply (50) to get

$$(51) \quad \|\delta\Phi_j\|_{1,\Omega} \leq c \|\delta u_1 - \delta u_2\|_{0,\Gamma} \leq c|\beta - \alpha| \|\delta p\|_{0,\Omega_0}, \quad j = 1, 2.$$

Subtracting (48) from (47), we have, for any $v \in V$,

$$\begin{aligned} & \int_{\Omega} [\nabla(\delta\Phi_1 - \delta\Phi_2) \cdot \nabla v + (\delta\Phi_1 - \delta\Phi_2)v] dx + \alpha \int_{\Gamma} (\delta\Phi_1 - \delta\Phi_2)v ds \\ &= (\beta - \alpha) \int_{\Gamma} \delta\Phi_2 v ds. \end{aligned}$$

Take $v = \delta\Phi_1 - \delta\Phi_2$ and apply (51) to obtain

$$(52) \quad \|\delta\Phi_1 - \delta\Phi_2\|_{1,\Omega} \leq c|\beta - \alpha| \|\delta\Phi_2\|_{0,\Gamma} \leq c(\beta - \alpha)^2 \|\delta p\|_{0,\Omega_0}.$$

Also, from (47) and by applying (51)–(52), we have

$$(53) \quad \|\alpha\delta\Phi_1 - \beta\delta\Phi_2\|_{1,\Omega} = \|(\alpha - \beta)\delta\Phi_1 + \beta(\delta\Phi_1 - \delta\Phi_2)\|_{1,\Omega} \leq c(\beta - \alpha)^2 \|\delta p\|_{0,\Omega_0}.$$

Since the projection operator is non-expansive ([2, Proposition 3.4.4]), we get from the definition (43) that

$$(54) \quad \|\Pi(p^1) - \Pi(p^2)\|_{0,\Omega_0} \leq \left\| \frac{1}{\varepsilon} (\alpha\delta\Phi_1 - \beta\delta\Phi_2) \right\|_{0,\Omega_0}.$$

Then apply (53),

$$\|\Pi(p^1) - \Pi(p^2)\|_{0,\Omega_0} \leq c\varepsilon^{-1}(\beta - \alpha)^2 \|\delta p\|_{0,\Omega_0}.$$

By the assumption (44),

$$(55) \quad \|\Pi(p^1) - \Pi(p^2)\|_{0,\Omega_0} \leq c c_0^2 \|p^1 - p^2\|_{0,\Omega_0}.$$

Thus, if $c_0 > 0$ is small enough, the mapping Π is a contraction from Q_{ad} to Q_{ad} , and we can apply the Banach fixed-point theorem to obtain the following result (cf. [2, Theorem 5.1.3]).

Theorem 4.1. *Assume (44) with a sufficiently small $c_0 > 0$. Then the system defined by (39)–(43) has a unique solution*

$$(p, u_1, u_2, \Phi_1, \Phi_2) \in Q_{ad} \times V^4.$$

Moreover, for any $p^0 \in Q_{ad}$, the iteration method $p^{n+1} = \Pi(p^n)$, $n \geq 0$, converges:

$$(p^n, u_1^n, u_2^n, \Phi_1^n, \Phi_2^n) \rightarrow (p, u_1, u_2, \Phi_1, \Phi_2) \in Q_{ad} \times V^4, \text{ as } n \rightarrow \infty.$$

Here, $u_1^n, u_2^n, \Phi_1^n, \Phi_2^n$ denote the solutions of the BVPs (39)–(42) with p replaced by p^n .

Note that the theorem provides a convergence result for the fixed point iteration method in solving the system (39)–(43).

5. Gradient projection method. In this section, a gradient projection iterative scheme for obtaining an approximation to p_ε , the solution of Problem 1, is stated. We first mention that p_ε is also characterized by a linear variational inequality (LVI):

$$\int_{\Omega_0} \left(p_\varepsilon - \frac{1}{\varepsilon} (\alpha\Phi_1 - \beta\Phi_2) \right) (q - p_\varepsilon) dx \geq 0 \quad \forall q \in Q_{ad}.$$

Applying the gradient projection method ([3, 4]) to LVI above, we introduce the following iterative scheme to compute an approximation of p_ε :

Algorithm 5.1.

1. Given precision $\epsilon > 0$ and data g_1, g_2 ; properly choose ϵ, α, β with $0 < \alpha < \beta$, and ρ ; Set $p^0 \in Q_{ad}$ and $n = 0$.
2. Solve (5) and (6), both with p_ϵ replaced by p^n to get $u_1(p^n)$ and $u_2(p^n)$.
3. Solve (9) and (10), both with $u_1(p_\epsilon) - u_2(p_\epsilon)$ replaced by $u_1(p^n) - u_2(p^n)$ to get $\Phi_1(p^n)$ and $\Phi_2(p^n)$.
4. Compute $g(p^n) = p^n - \frac{1}{\epsilon}(\alpha\Phi_1(p^n) - \beta\Phi_2(p^n))$.
5. Compute $p^{n+1} = P_{Q_{ad}}\left(p^n - \rho g(p^n)\right)$.
6. Compute $e^{n+1} = \|p^{n+1} - p^n\|_{0,\Omega_0}$. If $e^{n+1} \leq \epsilon$ stop; otherwise, set $n := n + 1$ and return to Step 2.

Convergence of Algorithm 5.1 can be studied similar to the fixed-point iteration, as stated in Theorem 4.1. Indeed, instead of (43), we define

$$(56) \quad \Pi(p) = P_{Q_{ad}}\left((1 - \rho)p + \frac{\rho}{\epsilon}(\alpha\Phi_1 - \beta\Phi_2)\right).$$

Instead of (54), we have

$$\|\Pi(p^1) - \Pi(p^2)\|_{0,\Omega_0} \leq \left\| (1 - \rho)\delta p + \frac{\rho}{\epsilon}(\alpha\delta\Phi_1 - \beta\delta\Phi_2) \right\|_{0,\Omega_0}$$

and then

$$(57) \quad \|\Pi(p^1) - \Pi(p^2)\|_{0,\Omega_0} \leq (1 - \rho)\|\delta p\|_{0,\Omega_0} + \frac{\rho}{\epsilon}\|\alpha\delta\Phi_1 - \beta\delta\Phi_2\|_{0,\Omega_0}.$$

The inequality (53) still holds and we use it in (57):

$$(58) \quad \|\Pi(p^1) - \Pi(p^2)\|_{0,\Omega_0} \leq [(1 - \rho) + c\rho\epsilon^{-1}(\beta - \alpha)^2]\|p^1 - p^2\|_{0,\Omega_0}.$$

Thus, for $\rho \in (0, 1)$, if $c_0 > 0$ in (44) is small enough, the mapping defined by (39)–(42) and (56) is a contraction, and the statement of Theorem 4.1 holds for this mapping. In particular, we have the convergence of Algorithm 5.1. Note that the the same convergence statement is valid also for the discrete version of the system. We comment that in numerical simulations, convergence occurs even for moderately large values of c_0 .

In practice, Q_{ad} often has one of three forms: (1) $Q_{ad} = Q$; (2) $Q_{ad} = \{p \in Q \mid p \geq 0 \text{ a.e. in } \Omega_0\}$; (3) $Q_{ad} = \{p \in Q \mid \underline{p} \leq p \leq \bar{p} \text{ a.e. in } \Omega_0\}$ with $\underline{p}, \bar{p} \in C(\bar{\Omega}_0)$. In these cases, $P_{Q_{ad}}$ has simple forms. Particularly, in the case $Q_{ad} = Q$, the iteration in Algorithm 5.1 can be avoided. In fact, in this case, $P_{Q_{ad}} = I$, the identical operator in Q , and $p_\epsilon = \frac{1}{\epsilon}(\alpha\Phi_1 - \beta\Phi_2)\chi_{\Omega_0}$. Substituting $\frac{1}{\epsilon}(\alpha\Phi_1 - \beta\Phi_2)\chi_{\Omega_0}$ for p back into (5) and (6), and together with (9) and (10), we arrive at a forward system of partial differential equations. Once Φ_1 and Φ_2 are computed from the reduced system, we obtain $p_\epsilon = \frac{1}{\epsilon}(\alpha\Phi_1 - \beta\Phi_2)\chi_{\Omega_0}$.

We note that all statements above hold for noise model in Section 3, just with g_1 and g_2 being replaced by g_1^δ and g_2^δ . In the next section, finite element methods will be used for obtaining discrete approximate solutions based on Algorithm 5.1 and some numerical experiments are presented.

6. Numerical experiments. In this section, some numerical results are reported based on our new reconstruction framework for the inverse source problem (1)–(2). Standard linear finite element methods are applied to obtain discrete approximate solutions of the BVPs. Let Ω be the problem domain and h be the mesh parameter, i.e., the maximal diameter of the elements in a partition \mathcal{T}_h of Ω . These results are computed in a Matlab environment. For a two dimensional domain, triangular

meshes are produced and refined by using of the PDE Toolbox. For a three dimensional domain, tetrahedral meshes are produced and refined through a COMSOL Multiphysics software. In all examples, biconjugate gradient (BICG) methods are used to solve the resulting linear algebraic system. The Dirichlet data g_1 , which may or may not include noise, are obtained by solving the forward BVP (1) on a rather fine mesh for a given true source p and Neumann data g_2 . Indicated by Proposition 3, without loss of generality, we set

$$\alpha = 1 \text{ and } \beta - \alpha = O(\sqrt{\varepsilon}) = \sqrt{m\varepsilon}$$

with m to be chosen. For better assessing the accuracy of approximate solutions, we define the L^2 -norm relative error in an approximate solution:

$$\text{Err}(p_\varepsilon^h) := \frac{\|p_\varepsilon^h - p\|_{0,\Omega_0}}{\|p\|_{0,\Omega_0}},$$

where p is the true source function, p_ε^h stands for an approximate solution of p_ε (for noise-free data) or p_ε^δ (for noise data).

Example 1. In this example, $\Omega = \{(x, y) \in \Omega \mid x^2 + y^2 < 1\}$, Ω_0 is a circle, centered at $(0.55, 0.45)$ with radius 0.2. The true source function $p(x, y) = 1 + x + y$ in Ω_0 . The Neumann data $g_2 = 0.2$ on Γ . Then Dirichlet data g_1 is computed through (1) on a mesh with $h = 0.0003278$, 351232 elements and 176177 nodes.

TABLE 1. $\text{Err}(p_\varepsilon^h)$ for noise-free data.

ε	HCW	SH	CGH
10^{-1}	0.8104	0.9201	0.9734
10^{-2}	0.2953	0.5339	0.8018
10^{-3}	0.03261	0.09746	0.3467
10^{-4}	0.02444	0.003205	0.08941
10^{-5}	0.1017	0.04778	0.03773
10^{-6}	0.2314	0.1500	0.03114
10^{-7}	0.7288	0.3214	0.03056
10^{-8}	1.700	0.9816	0.03068
10^{-9}	4.541	1.857	0.03066
10^{-10}	8.972	5.531	0.03078
10^{-11}	19.66	9.488	0.03061
10^{-12}	48.02	64.75	0.03348

We consider first the case where the source function p is searched in the whole space Q , i.e., $Q_{ad} = Q$. For fixed $m = 10^5$, reconstruction is repeated on a mesh with $h = 0.02134$, 1372 elements and 722 nodes for different ε , and L^2 -norm relative errors in approximate source functions are reported in fourth column of Table 1. For comparison with methods in [7] and [12], approximate source functions are also computed with these two methods. The associated L^2 -norm relative errors are listed in the second and third columns of Table 1 respectively. In Table 1, symbols ‘HCW’, ‘SH’ and ‘CGH’ mean that results in the corresponding column are obtained with reconstruction models (3), (4) and (7), respectively. Table 1 shows that all the three methods perform well for properly selected parameters. We conclude from Table 1

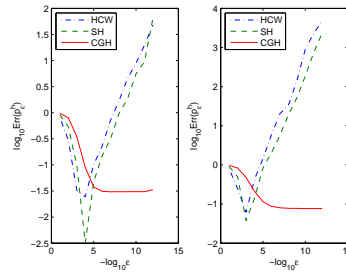


FIGURE 1. Left subgraph: noise-free case; right subgraph: noise case.

that, although Proposition 3 is discussed for accurate p_ε , it also holds for p_ε^h , that is, p_ε^h is uniform with respect to ε when ε is small enough. In other words, with our new method, a reasonable source function can be reconstructed for rather small regularization parameter ε . It is meaningful by noticing the fact that the smaller ε is, the better the regularized problem approaches to the original one is. As a result, without the need for concern of possible instability associated with a very small ε , in our new method, we can choose a small value of ε based on the consideration of the solution accuracy, and the method will work as long as $\beta - \alpha$ is small enough.

TABLE 2. $\text{Err}(p_\varepsilon^h)$ for 5% noise data.

ε	HCW	SH	CGH
10^{-1}	0.7973	0.9146	0.9742
10^{-2}	0.2467	0.5016	0.8319
10^{-3}	0.06167	0.03798	0.4792
10^{-4}	0.4263	0.1401	0.2117
10^{-5}	1.440	0.8318	0.1147
10^{-6}	5.857	2.019	0.08748
10^{-7}	20.38	5.600	0.08008
10^{-8}	33.50	19.11	0.07780
10^{-9}	141.3	51.64	0.07730
10^{-10}	905.5	186.2	0.07686
10^{-11}	2296	746.7	0.07683
10^{-12}	4825	2353	0.07686

To measure the stability of the new K-V type reconstruction model, 5% uniformly distributed noise is added to g_1 . Set $m = 10^4$. The above experiments are repeated, and the resulting approximate solution errors are shown in the fourth column of Table 2. Counterpart with methods in [7] and [12] are also computed, and shown in the second and third columns. Table 2 shows that the results for model with noise are similar to those for noise-free case: $\frac{1}{\varepsilon}(\alpha\Phi_1^\delta - \beta\Phi_2^\delta)$ is uniform with respect to ε for small enough ε ; with properly selectly α and β , reasonable approximate source functions could be obtained for rather small ε . More importantly, we can see from it that the reconstruction model is stable. For clarity, Tables 1 and 2 are plotted in

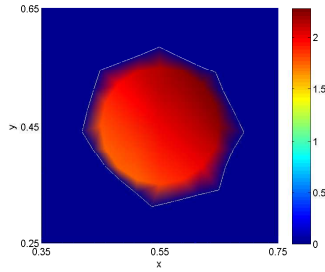
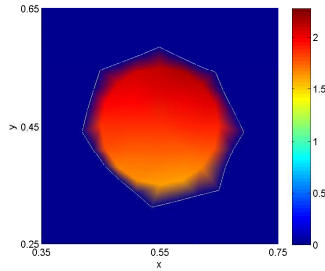
FIGURE 2. p_ε^h for noise-free model.FIGURE 3. p_ε^h for 5% noise model.

Figure 1. Finally, we show in Figures 2 and 3 the approximate source function p_ε^h with the best accuracy. Specifically, Figure 2 is p_ε^h for $\delta = 0, \varepsilon = 10^{-7}$ and $m = 10^5$; Figure 3 is p_ε^h for $\delta = 0.05, \varepsilon = 10^{-11}$ and $m = 10^4$.

Example 2. In this example, a 3D source is reconstructed. For this purpose, set the problem domain Ω :

$$\bar{\Omega} = \{(x, y, z) \mid x^2 + y^2 \leq 100, 0 \leq z \leq 10\}.$$

Assume Ω_0 is sphere centered at $(5, 5, 6)$ with unit radius and we place a true source $p = 5$ in $\bar{\Omega}_0$. Then for given $g_2 = |\sin(x + y + z)|$, (1) is used to compute measurement g_1 , on a mesh with $h = 0.1355$, 162759 tetrahedrons and 29043 nodes. A sketch of computational mesh is shown in Figure 4.

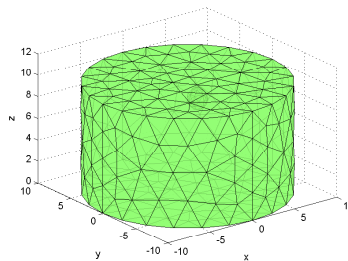


FIGURE 4. A sketch of computation mesh.

With $m = 10^3$, Algorithm (5.1) is used again to obtain approximate source functions for different ε on a mesh with $h = 0.2210$, 8463 tetrahedrons and 1656 nodes. We list the L^2 -norm relative errors, computed with methods in [7], [12] and this paper respectively, in Table 3. As 2D example above, for the 3D problem, similar conclusions can be drawn from Table 3.

TABLE 3. $\text{Err}(p_\varepsilon^h)$ for noise-free data.

ε	HCW	SH	CGH
10^{-1}	0.6362	0.6656	0.7292
10^{-2}	0.07430	0.08240	0.3657
10^{-3}	0.1475	0.1785	0.1709
10^{-4}	0.2386	0.2586	0.1070
10^{-5}	0.4192	0.4494	0.08777
10^{-6}	0.5078	0.6657	0.08193
10^{-7}	0.5207	0.7128	0.08013
10^{-8}	0.5216	0.7171	0.07952
10^{-9}	0.5221	0.7181	0.07933
10^{-10}	0.5216	0.7186	0.07928
10^{-11}	0.5215	0.7182	0.07926
10^{-12}	0.5224	0.7191	0.07925

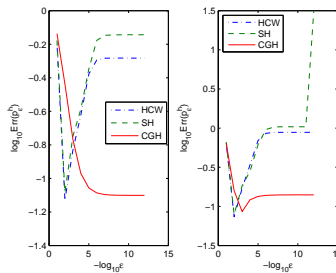


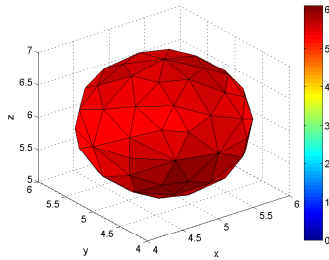
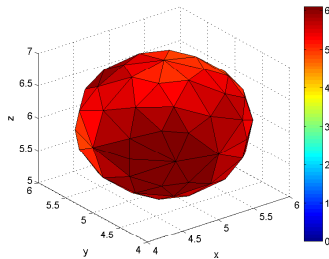
FIGURE 5. Left subgraph: noise-free case; right subgraph: noise case.

Again, for verifying the stability of our formulation, 5% random noise is added to Dirichlet data g_1 . Set $m = 10^4$, reconstruction above is repeated for this 3D problem. Approximate solution errors are shown in Table 4. Again, we plot Tables 3 and 4 in Figure 5. Finally, the approximate source function p_ε^h with the best accuracy for noise-free model and 5% noise model are displayed in Figures 6 and 7, respectively. Specifically, Figure 6 is p_ε^h for $\delta = 0, \varepsilon = 10^{-3}$ and $m = 10^4$ while Figure 7 is p_ε^h for $\delta = 0.05, \varepsilon = 10^{-3}$ and $m = 10^4$. Conclusion could be drawn from these results that the model explored here is stable.

We note that all numerical results above are obtained for Case 1: $Q_{ad} = Q$. Using Algorithm 5.1, we repeat the experiments for Case 2: $Q_{ad} = \{p \in Q \mid p \geq 0 \text{ a.e. in } \Omega_0\}$ and Case 3: $Q_{ad} = \{p \in Q \mid \underline{p} \leq p \leq \bar{p} \text{ a.e. in } \Omega_0\}$, and the reconstructed results are similar to those for Case 1. In summary, we conclude from them that the method proposed here is feasible and effective.

TABLE 4. $\text{Err}(p_\varepsilon^h)$ for 5% noise data.

ε	HCW	SH	CGH
10^{-1}	0.6355	0.6645	0.6417
10^{-2}	0.07348	0.07901	0.1582
10^{-3}	0.1699	0.1834	0.08592
10^{-4}	0.3410	0.2818	0.1216
10^{-5}	0.6943	0.6155	0.1340
10^{-6}	0.8573	0.9584	0.1383
10^{-7}	0.8804	1.032	0.1397
10^{-8}	0.8829	1.041	0.1402
10^{-9}	0.8833	1.041	0.1403
10^{-10}	0.8835	1.041	0.1404
10^{-11}	0.8824	1.041	0.1402
10^{-12}	0.8841	30.94	0.1404

FIGURE 6. p_ε^h for noise-free model.FIGURE 7. p_ε^h for 5% noise model.

7. Concluding remarks. In this paper, a new Kohn-Vogelius type formulation is proposed for the inverse source problem of elliptic PDEs. Different from existing methods in the literature, we introduce two positive parameter to form two different but related BVPs, so that the original boundary fitting is transferred to domain fitting. With two new BVPs, the boundary measurement is incorporated

into Robin boundary condition. From the practical point of view, this is meaningful since the effects of noise in forward boundary condition and noise in measurement on solution accuracy are different. The most important feature of the new method is that an accurate approximate source function can be reconstructed for rather small regularization parameter, even in the case where the data is polluted by random noise. Therefore, although in standard regularization methods for the inverse source problem, choosing a proper regularization parameter is delicate issue, our new method allows the use of a very small regularization parameter based mostly on the consideration of the solution accuracy.

Acknowledgments. We thank the two anonymous referees for their careful review of our manuscript and for their constructive comments. The work of the first author was supported by the Key Project of the Major Research Plan of NSFC (Grant No. 91130004). The work of the second author was supported by the Natural Science Foundation of China (Grant No. 11401304), the Natural Science Foundation of Jiangsu Province (Grant No. BK20130780), and the Fundamental Research Funds for the Central Universities (Grant No. NS2014078). The work of the third author was partly supported by Simons Foundation (Grant No. 207052 and 228187).

REFERENCES

- [1] L. Afraites, M. Dambrine and D. Kateb, [Conformal mappings and shape derivatives for the transmission problem with a single measurement](#), *Numer. Func. Anal. Opt.*, **28** (2007), 519–551.
- [2] K. Atkinson and W. Han, *Theoretical Numerical Analysis: A Functional Analysis Framework*, 3rd edition, Springer-Verlag, New York, 2009.
- [3] D. P. Bertsekas and E. M. Gafni, Projection method for variational inequalities with applications to the traffic assignment problem, *Math. Prog. Study*, **17** (1982), 139–159.
- [4] R. W. Cottle, F. Giannessi and J. L. Lions, *Variational Inequalities and Complementarity Problems: Theory and Applications*, John Wiley and Sons, New York, 1980.
- [5] L. C. Evans, *Partial Differential Equations*, American Mathematical Society, 1998.
- [6] P. Grisvard, *Elliptic Problems in Nonsmooth Domains*, Pitman, Boston, 1985.
- [7] W. Han, W. X. Cong and G. Wang, [Mathematical theory and numerical analysis of bioluminescence tomography](#), *Inverse Probl.*, **22** (2006), 1659–1675.
- [8] W. Han, K. Kazmi, W. X. Cong and G. Wang, [Bioluminescence tomography with optimized optical parameters](#), *Inverse Probl.*, **23** (2007), 1215–1228.
- [9] V. Isakov, *Inverse Problems for Partial Differential Equations*, Springer, New York, 1998.
- [10] J. L. Lions, *Optimal Control of Systems Governed by Partial Differential Equations*, Springer-Verlag, Berlin, 1971.
- [11] C. Qin, J. Feng, S. Zhu, X. Ma, J. Zhong, P. Wu, Z. Jin and J. Tian, [Recent advances in bioluminescence tomography: Methodology and system as well as application](#), *Laser Photon. Rev.*, **8** (2014), 94–114.
- [12] S. J. Song and J. G. Huang, Solving an inverse problem from bioluminescence tomography by minimizing an energy-like functional, *J. Comput. Anal. Appl.*, **14** (2012), 544–558.
- [13] A. N. Tikhonov and V. Y. Arsenin, *Solutions of Ill-Posed Problems*, Wiley, New York, 1977.

Received October 2014; revised May 2015.

E-mail address: xiaoliangcheng@zju.edu.cn

E-mail address: grf_math@nuaa.edu.cn

E-mail address: weimin-han@uiowa.edu